

Implementation of a Digital Signal Processor-controlled Shunt Active Filter

L. R. LIMONGI, M. C. CAVALCANTI, F. A. S. NEVES, G. M. S. AZEVEDO

UFPE. Recife - PE - Brasil, Brasile

Summary: This paper presents the implementation of an active filter configuration for harmonic compensation. The system can be controlled for current harmonics and reactive power compensations simultaneously by using a converter operating as active shunt filter. A synchronous reference frame based controller is compared to an instantaneous reactive power based controller. The synchronous reference frame method is chosen to control the converter due to the better performance when the supply voltage is distorted. A shunt active filter system has been designed and built to meet IEEE 519 recommended harmonic standards. Simulation demonstrates the good performance of the active filter configuration. Experimental results, corresponding to the operation of the digital signal processor-controlled shunt active filter are also presented.

Keywords:
active filters,
current control,
power quality

1. INTRODUCTION

Strict regulations have been applied to equipments connected to the grid. Some of these regulations are related to harmonics distortion and power factor. However, with the development of power electronics, many equipments tend to increase the levels of harmonic distortion. For example, the supply current at the input of a diode bridge rectifier deviates significantly from a sinusoidal waveform and this distorted current can also lead to distortion in the supply voltage. Moreover, many modern equipments use digital controllers, based on microprocessors sensitive to variations in the voltage and current waveforms.

The first attempt to overcome the effects of the non-linear loads appeared with the use of passive filters (L-C filter). However, implementing them brought some problems:

- The supply impedance is unknown and it strongly influences the compensation characteristics of the passive filter.
- It may cause resonance with the supply at some frequencies.

As a consequence of these items above, passive filters designs requires extensive system studies and considerable engineering efforts [1].

With the advent of fast commutating switches, the Active Filters (*AFs*) appeared as a better way to eliminate harmonics related problems and it is becoming a cost effective solution. A shunt *AF* is a good solution to compensate current harmonics. However, operation performance of the shunt *AF* system is strongly dependent on the algorithm employed to control the inverter. It has been shown that synchronous reference frame (*SRF*) controller and instantaneous reactive power (*IRP*) theory based compensators achieve good performance for implementation.

On the other hand, the rising complexity of power electronics applications and their control techniques require an increasing use of microcontrollers and digital signal processors (*DSP*). The *DSP* is a device that manipulates digital data with the objective of generating control signals in real time. With the recent advance of technology, the use

of *DSP* have becoming cost competitive and it will be only a matter of time for these chips totally replace the conventional analog control circuits.

The purpose of this paper is to present a shunt *AF* system for connection in a three-phase system. The *AF* provides the functions of current harmonic and reactive power compensations. A *SRF* is compared to an *IRP* based method. A *DSP* is used to implement the control of the shunt *AF* using the *SRF* method.

2. ACTIVE FILTERS

An *AF* can be classified in four categories in according to its topology [2]. It can be used as series, shunt, combination of both, or with passive and active filters together (called hybrid configuration), as shown in Figure 1.

A series *AF* is usually employed to suppress voltage harmonics, voltage flicker and to decrease the voltage unbalance in three-phase systems.

A shunt *AF* is a suitable device for current-based compensation [3, 4]. This configuration includes current harmonics and reactive power compensations.

The combination of these topologies (series and shunt) is called Unified Power Quality Conditioner (*UPQC*) [5]. The *UPQC* is expected to be one of the best solutions for active filtering, since it joins the main characteristics of series and shunt filter. The weak point of this kind of filter is the use of two converters with the consequence of increasing costs.

An alternative solution for the budget problems of *UPQC* is the hybrid filter. This filter configuration is used with a series *AF* (working as a harmonic isolator) and a shunt passive filter to eliminate the current harmonics [6–9]. The series *AF* isolates the supply impedance from the passive filter avoiding resonances.

The *AFs* can be implemented with a current source converter or a voltage source converter. The voltage source converter is widely employed because it usually presents higher efficiency than the current source converter.

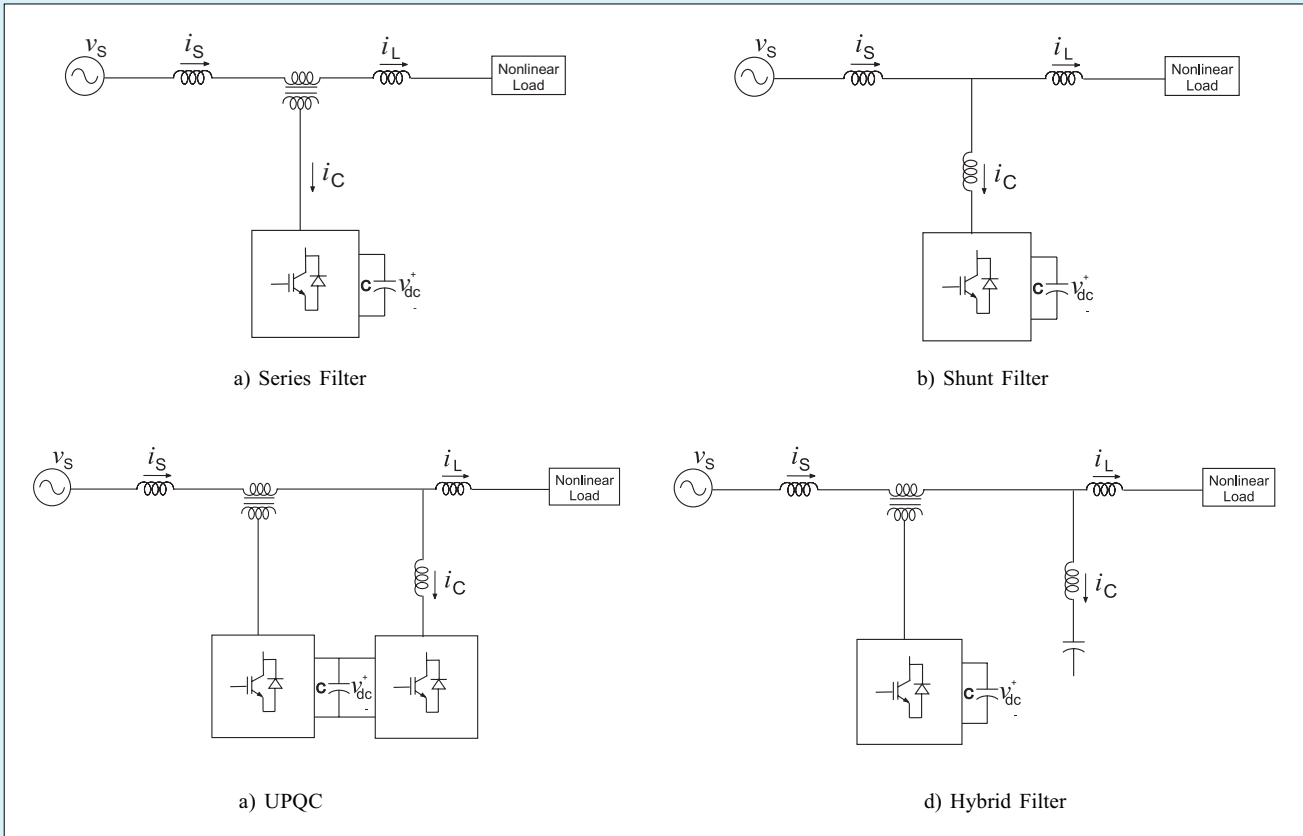


Fig. 1. Active filters topologies

The AFs can also be classified based on the numbers of phases. If the filter is being used on a single phase system the AFs can be classified as two-wire configurations, and if the filter is connected to a three phase system the AFs can be classified in three wire or four wire configurations.

3. SHUNT ACTIVE FILTER

The compensation characteristics of a shunt active filter are based on injecting currents in the system with the same amplitude and reverse phase of the load harmonics and/or reactive currents components at the point of connection, in order to cancel them.

The compensations capabilities of a shunt AF includes:

- Current harmonic injection
- Unbalanced load current compensation
- Resonance damping
- Reactive power production

The shunt active filter shown in Figure 2 is modeled in the stationary abc reference frame as described in [3, 10]:

$$\frac{d}{dt} \begin{bmatrix} i_a \\ i_b \\ v_{dc} \end{bmatrix} = \begin{bmatrix} -\frac{R_c}{L_c} & 0 & -\frac{d_{na}}{L_c} \\ 0 & -\frac{R_c}{L_c} & -\frac{d_{nb}}{L_c} \\ \frac{2d_{na} + d_{nb}}{C} & \frac{d_{na} + d_{nb}}{C} & 0 \end{bmatrix} \begin{bmatrix} i_a \\ i_b \\ v_{dc} \end{bmatrix} + \frac{1}{L_c} \begin{bmatrix} v_a \\ v_b \\ 0 \end{bmatrix} \quad (1)$$

where:

- i_a, i_b — two of the three-phase inverter currents;
- v_{dc} — dc link voltage;
- R_c, L_c — resistance and inductance of transformer;
- d_{na}, d_{nb}, d_{nc} — three-phase switching state functions;
- C — capacitance of the dc link;
- v_a, v_b, v_c — three-phase supply voltages.

A. Modeling the SRF control of shunt filter

The AF of Figure 2 can be modeled in the rotating dq reference frame from (1) with the aim of reducing control complexity if compared with the control using the stationary abc reference frame model.

In order to convert quantities from abc to an arbitrary rotating $dq0$ reference frame, the transformation matrix is necessary:

$$T_{dq0}^{abc} = \sqrt{\frac{2}{3}} \begin{bmatrix} \cos(\omega t) & \cos\left(\omega t - \frac{2\pi}{3}\right) & \cos\left(\omega t - \frac{4\pi}{3}\right) \\ -\sin(\omega t) & -\sin\left(\omega t - \frac{2\pi}{3}\right) & -\sin\left(\omega t - \frac{4\pi}{3}\right) \\ \frac{1}{\sqrt{2}} & \frac{1}{\sqrt{2}} & \frac{1}{\sqrt{2}} \end{bmatrix} \quad (2)$$

A Phased Locked Loop (PLL) scheme is used to determine the angle for the dq reference frame orientation such that $v_q = 0$ and $v_d = \sqrt{3/2}\hat{V}$, assuming the supply voltage is given by (3).

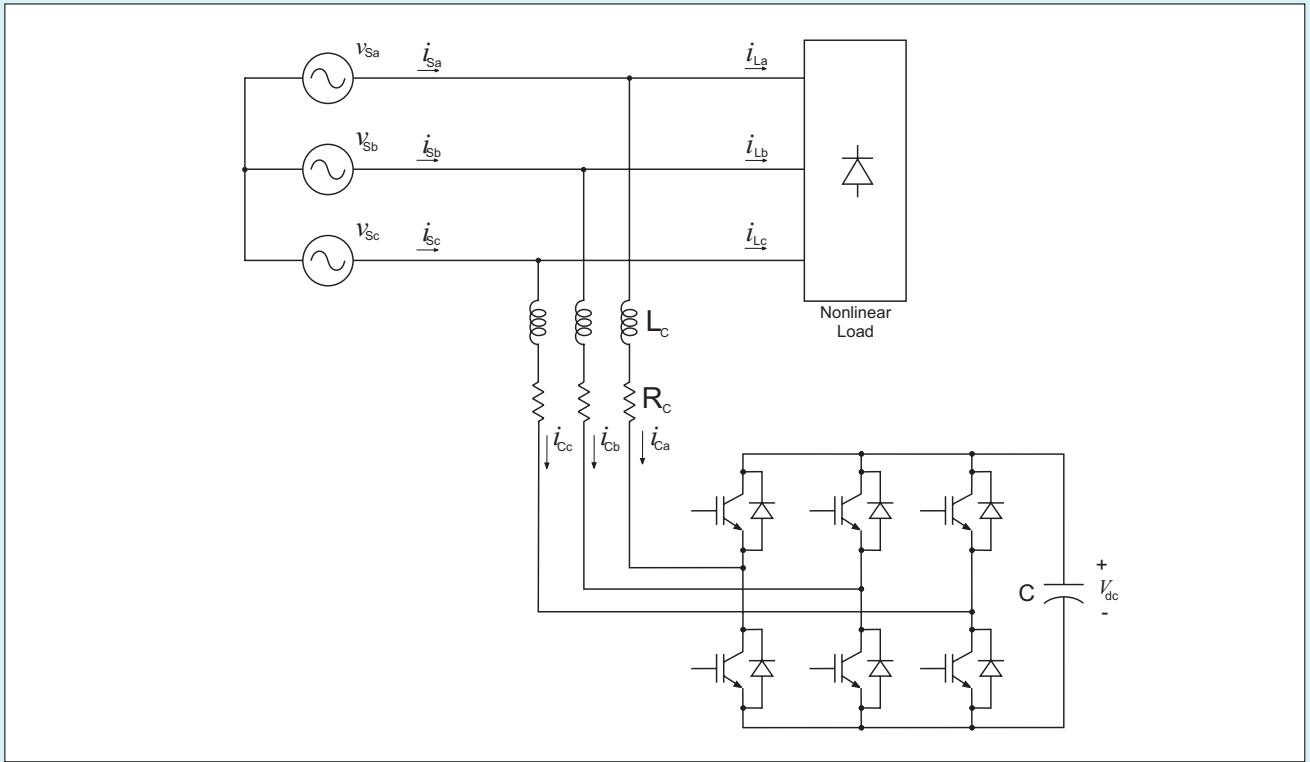


Fig. 2. Shunt active filter with a voltage source inverter.

$$\begin{aligned} v_a &= \hat{V} \cos(\omega t) \\ v_b &= \hat{V} \cos(\omega t - 2\pi/3) \\ v_c &= \hat{V} \cos(\omega t - 4\pi/3) \end{aligned} \quad (3)$$

In steady-state conditions the fundamental component of dq quantities is constant. To impose the harmonics on the inverter of Figure 2 it is necessary to separate the constant current component from the oscillating component. This oscillating component with reverse phase is the reference of the controller.

The dynamic model, which is described in [3] and [10], of the system in dq reference frame is obtained from equations (1) and (2) resulting in:

$$\frac{d}{dt} \begin{bmatrix} i_d \\ i_q \\ v_{dc} \end{bmatrix} = \begin{bmatrix} -\frac{R_c}{L_c} & \omega & -\frac{d_{nd}}{L_c} \\ \omega & -\frac{R_c}{L_c} & -\frac{d_{nq}}{L_c} \\ \frac{d_{nd}}{C} & \frac{d_{nq}}{C} & 0 \end{bmatrix} \begin{bmatrix} i_d \\ i_q \\ v_{dc} \end{bmatrix} + \frac{1}{L_c} \begin{bmatrix} v_d \\ v_q \\ 0 \end{bmatrix} \quad (4)$$

where d_{nd} and d_{nq} are the switching state functions of the system in dq reference frame and ω is the supply angular frequency. The first and second lines of the model can be written as:

$$L_c \frac{di_d}{dt} + R_c i_d = L_c \omega i_q - v_{dc} d_{nd} + v_d \quad (5)$$

$$L_c \frac{di_q}{dt} + R_c i_q = -L_c \omega i_d - v_{dc} d_{nq} + v_q \quad (6)$$

Let u_d and u_q be the right side terms of equations (5) and (6):

$$u_d = L_c \omega i_q - v_{dc} d_{nd} + v_d \quad (7)$$

$$u_q = -L_c \omega i_d - v_{dc} d_{nq} + v_q \quad (8)$$

The terms u_d and u_q are the respective outputs of the two current PI controllers:

$$u_d = K_p \tilde{i}_d + K_i \int \tilde{i}_d dt \quad (9)$$

$$u_q = K_p \tilde{i}_q + K_i \int \tilde{i}_q dt \quad (10)$$

where $\tilde{i}_d = i_d^* - i_d$ and $\tilde{i}_q = i_q^* - i_q$ are the current errors.

With the equations (7) and (8) the switching state functions (11) and (12) can be found.

$$d_{nd} = \frac{v_d + L_c \omega i_q - u_d}{v_{dc}} \quad (11)$$

$$d_{nq} = \frac{v_q + L_c \omega i_d - u_q}{v_{dc}} \quad (12)$$

The terms $\frac{v_d + L_c \omega i_q}{v_{dc}}$ and $\frac{v_q + L_c \omega i_d}{v_{dc}}$ in (11) and (12) are called compensation parts and they can be added (or not) to the output of the PI controllers.

The third equation of the model (4) is given by:

$$C \frac{v_{dc}}{dt} = d_{nd}i_d + d_{nq}i_q \quad (13)$$

This equation can be rewritten as:

$$u_{dc} = d_{nd}i_d + d_{nq}i_q \quad (14)$$

In order to control the dc voltage, a PI controller is used:

$$u_{dc} = K_{pv}\tilde{v}_{dc} + K_{iv}\int\tilde{v}_{dc}dt \quad (15)$$

where $\tilde{v}_{dc} = v_{dc}^* - v_{dc}$ is the voltage error. The control effort is obtained from equation (16).

$$i_{do}^* = \frac{u_{dc} - d_{nq}i_q}{d_{nd}} = \frac{u_{dc}v_{dc} - d_{nq}i_qv_{dc}}{d_{nd}v_{dc}} \quad (16)$$

Assuming that the current loop is ideal, the following properties hold:

$$\begin{aligned} d_{nq}v_{dc} &\approx v_q \\ d_{nd}v_{dc} &\approx v_d \end{aligned} \quad (17)$$

Assuming the supply voltage is given by equation (3) the transformation of v_a and v_b to dq coordinates yields $v_d = \sqrt{3}/2\hat{V}$ and $v_q = 0$. As a result, $d_{nq}v_{dc} \approx v_q = 0$ and $d_{nd}v_{dc} \approx v_d = \sqrt{3}/2\hat{V}$. The control effort can be approximated by:

$$i_{do}^* = \sqrt{\frac{2}{3}} \frac{v_{dc}}{\hat{V}} u_{dc} \quad (18)$$

The instantaneous active power is $p = v_d i_d$. In order to maintain the dc link voltage, the d-axis current in (18) must be added to i_d^* , because the i_q current does not contribute for the active power to maintain the dc link voltage.

B. Modeling the IRP control of shunt active filter

The conventional theory of active and reactive power fails if the system is unbalanced and distorted. Additionally this theory only works in steady state conditions. Akagi [11, 12] proposed the theory of instantaneous active and reactive power with the intention of developing the control of active filters.

The current control scheme is done in $\alpha\beta 0$ coordinates as in Figure 4. The transformation of the currents i_a, i_b, i_c to i_α, i_β, i_0 is given by:

$$\begin{bmatrix} i_\alpha \\ i_\beta \\ i_0 \end{bmatrix} = \sqrt{\frac{2}{3}} \begin{bmatrix} 1 & -1/2 & -1/2 \\ 0 & \sqrt{3}/2 & -\sqrt{3}/2 \\ 1/\sqrt{2} & 1/\sqrt{2} & 1/\sqrt{2} \end{bmatrix} \begin{bmatrix} i_a \\ i_b \\ i_c \end{bmatrix} \quad (19)$$

The IRP theory defines the instantaneous real power p and p_0 , and the instantaneous imaginary power q as follows [13]:

$$\begin{bmatrix} p_0 \\ p \\ q \end{bmatrix} = \begin{bmatrix} v_0 & 0 & 0 \\ 0 & v_\alpha & v_\beta \\ 0 & v_\beta & -v_\alpha \end{bmatrix} \begin{bmatrix} i_0 \\ i_\alpha \\ i_\beta \end{bmatrix} \quad (20)$$

where:

- i_α, i_β — α -axis and β -axis current components;
- i_0 — zero-sequence current component.
- v_α, v_β — α -axis and β -axis voltage components.
- v_0 — Zero-sequence voltage component.

The active and reactive power is given as following:

$$P_{active} = v_\alpha i_\alpha + v_\beta i_\beta + v_0 i_0 = p + p_0 \quad (21)$$

$$P_{reactive} = v_\beta i_\alpha - v_\alpha i_\beta \quad (22)$$

The reactive power exists in all phases individually but vanishes when added. In other words it does not give any contribution of active powers on the entire three phase system.

Considering that the system is unbalanced and distorted the active and reactive instantaneous power is composed of average and oscillating components.

$$\begin{aligned} p &= \bar{p} + \tilde{p} \\ q &= \bar{q} + \tilde{q} \\ p_0 &= \bar{p}_0 + \tilde{p}_0 \end{aligned} \quad (23)$$

The control of shunt active filter using the IRP theory is based on the separation of the average from the oscillating part of components p and q considering a balanced system. This consideration eliminates the p_0 components. Using a simple high-pass filter we can separate these components and determine the reference currents as follows:

$$\begin{bmatrix} i_\alpha \\ i_\beta \end{bmatrix} = \frac{1}{v_\alpha^2 + v_\beta^2} \begin{bmatrix} v_\alpha & v_\beta \\ v_\beta & -v_\alpha \end{bmatrix} \begin{bmatrix} \tilde{p} \\ \tilde{q} \end{bmatrix} \quad (24)$$

From the abc dynamic model of (1) and using the matrix transformation of equation (19), the whole model in $\alpha\beta$ coordinates derives as following:

$$\frac{d}{dt} \begin{bmatrix} i_\alpha \\ i_\beta \\ v_{dc} \end{bmatrix} = \begin{bmatrix} -\frac{R_c}{L_c} & 0 & -\frac{d_{n\alpha}}{L_c} \\ 0 & -\frac{R_c}{L_c} & -\frac{d_{n\beta}}{L_c} \\ \frac{d_{n\alpha}}{C} & \frac{d_{n\beta}}{C} & 0 \end{bmatrix} \begin{bmatrix} i_\alpha \\ i_\beta \\ v_{dc} \end{bmatrix} + \frac{1}{L_c} \begin{bmatrix} v_\alpha \\ v_\beta \\ 0 \end{bmatrix} \quad (25)$$

By using this model, one can develop the expressions for the switching state function in $\alpha\beta$ coordinates in the same manner as in (11) and (12). The expressions are:

$$d_{n\alpha} = \frac{v_\alpha - v_\alpha}{v_{dc}} \quad (26)$$

$$d_{n\beta} = \frac{v_\beta - v_\beta}{v_{dc}} \quad (27)$$

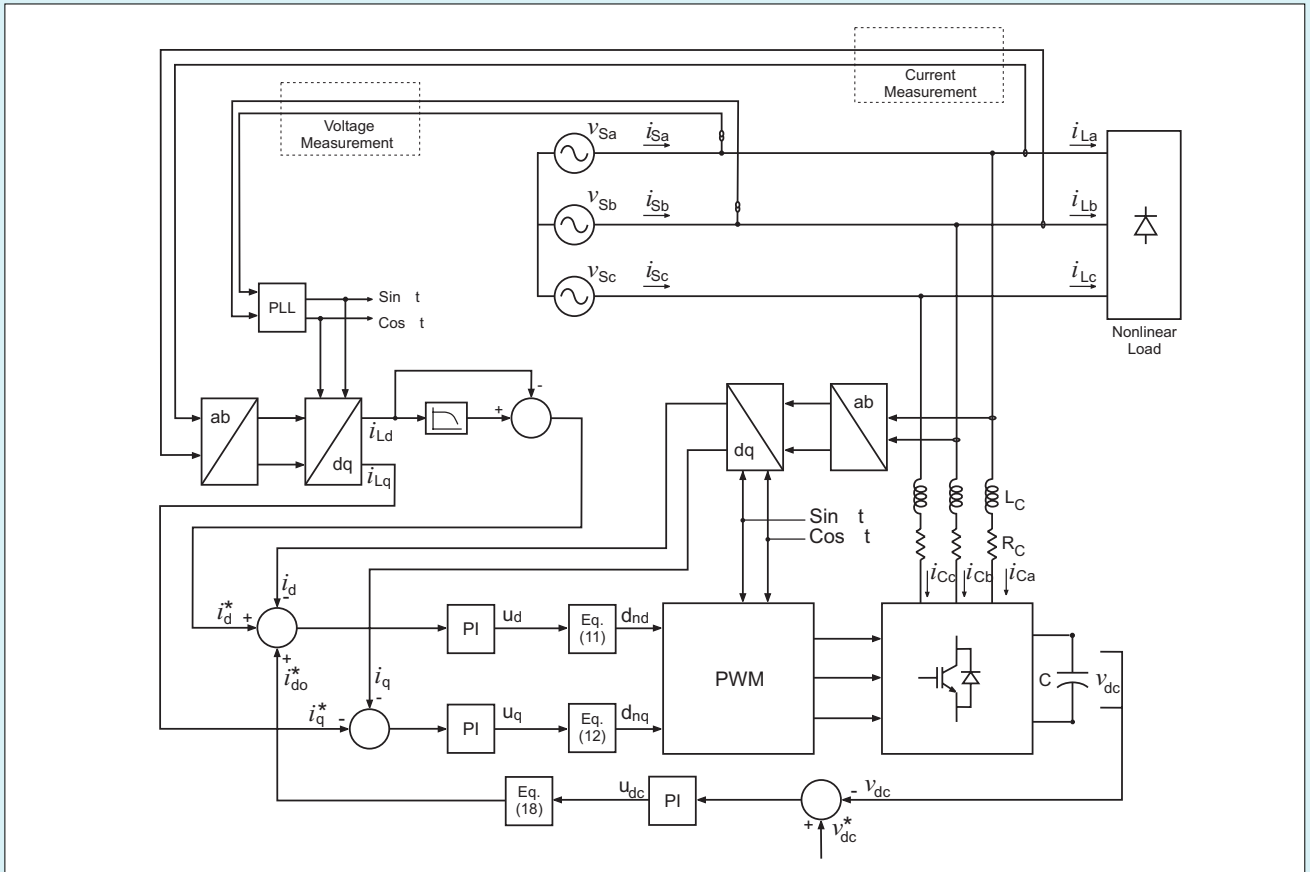


Fig. 3. Schematic diagram of shunt active filter with SRF based controller

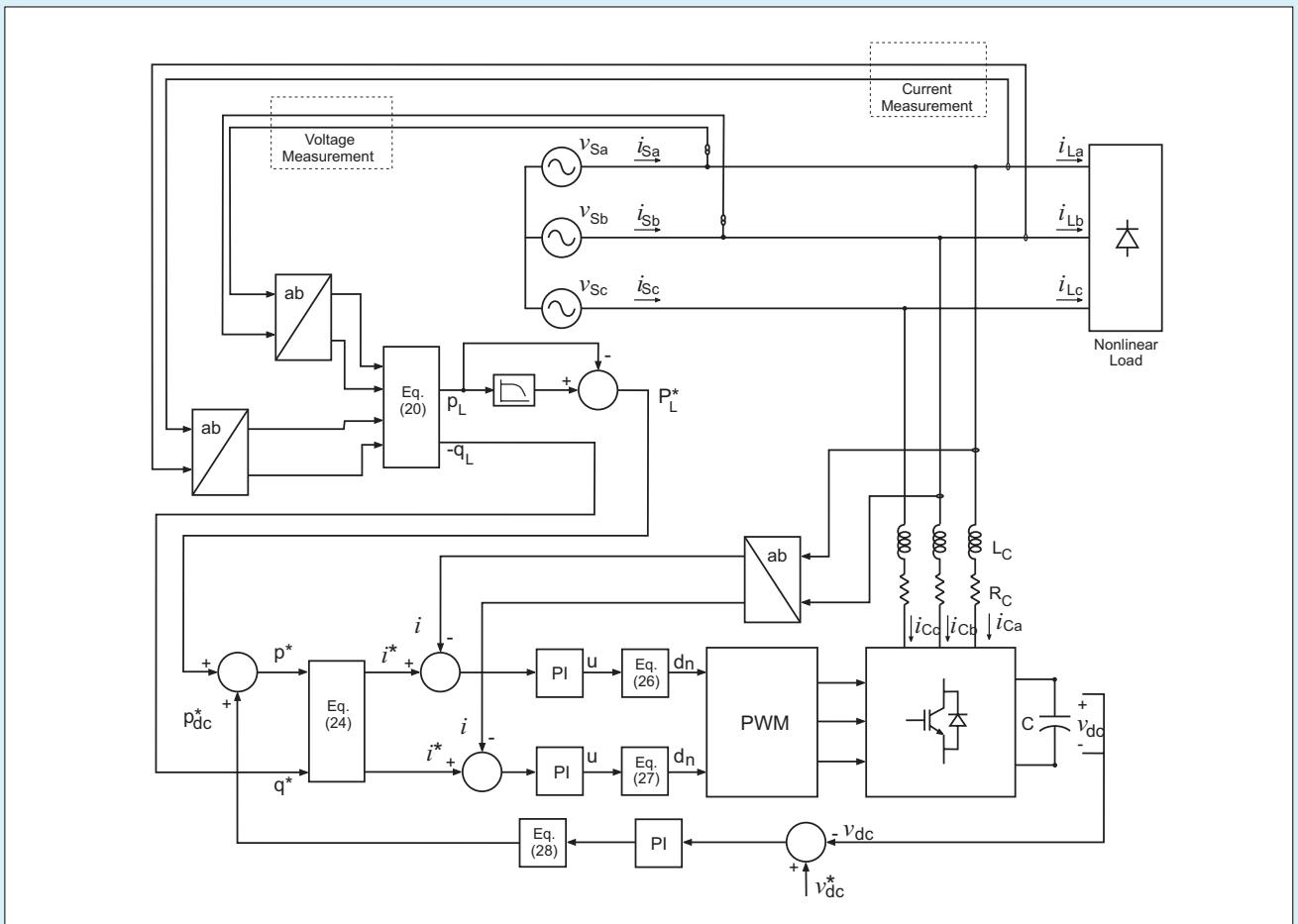


Fig. 4. Schematic diagram of shunt active filter with IRP based controller.

The power reference to maintain the dc link voltage is given by:

$$P_{dc}^* = v_{dc} u_{dc} \quad (28)$$

4. SIMULATION RESULTS

The both systems of Figure 3 and Figure 4 were simulated in *Matlab* with the parameters shown in Table 1. If the three-phase supply voltage is balanced and undistorted, the *SRF* based controller and the *IRP* based controller can compensate current harmonic and reactive power effectively. The *THD* of the supply current under these conditions is 3.92% for *SRF* based controller and is 3.93% for the *IRP* based controller. The relevant waveforms are presented in Figure 6.

Based on results, the criteria to be used to compare the controllers is the operation under distorted supply voltage. The *SRF* based controller is almost insensitive to supply voltage distortions, since any non-dc component in the *SRF* can be attributed to harmonics in steady-state [14].

The *IRP* based controller has problems with the supply voltage distortion, since the product of supply voltage and load current will result in real power contained at the harmonic frequencies. This real power contained at harmonic frequencies will result in a distorted supply current [14].

Table 1. System Parameters

Conditions	SRF	IRP
Supply RMS voltage	220	220
Transformer	220/16.3V	220/16.3V
Inductance	1.8mH	1.8mH
Capacitance	4.7mF	4.7mF
Load impedance	40 ohms	40 ohms
Dc link reference voltage	100	100
Current loop integral gain	10	20
Current loop proporcional gain	50	400
Voltage loop integral gain	0.5	1
Voltage loop proporcional gain	1.5	40
PWM technique	SVPWM	SVPWM

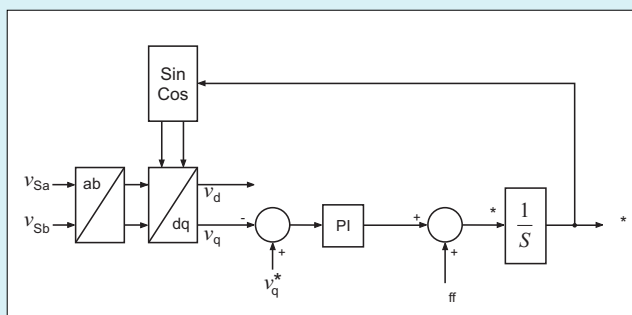


Fig. 5. Phased Locked Loop

The simulation results show that the *SRF* method presents better performance than the *IRP* when the supply voltage is distorted (Fig. 7). The *THD* of supply current is 5.15% for the *SRF* based controller and is 5.85% for the *IRP* based controller.

The performance of *SRF* method can be improved if the characteristics of the *PLL* (5) are changed. The *PLL* used in *SRF* method under non distorted supply voltage yields to good results. However, under distorted supply voltage, the reference angle in the output of *PLL* contribute to increase the distortion on the supply current since the ideal angle can not be tracked by the *PLL*. The high bandwidth of the *PLL* increases the problems related to voltages distortions, resulting in more harmonics in the supply current. To reduce the effects of these harmonics, the *PLL* bandwidth can be reduced [15]. In fact, the frequency of supply voltage does not change substantially, then a small bandwidth will achieve good results for the *PLL* output.

Decreasing the bandwidth of the *PLL*, the current distortion changes to 4.37%. Using this bandwidth condition, the current distortion under non distorted voltage supply is 4.35%. Assuming that voltage distortions are very common on the utility, it is better to project the gains of the *PLL*, considering a small bandwidth.

Figures 8(a) and 8(b) show the *PLL* response for two different bandwidth. It can be seen that the voltage from the *PLL* reference angle in Figure 8(a) presents lower distortion than the voltage in Figure 8(b). The first case (Fig. 8(a)) was simulated with a bandwidth of 50Hz and the second case (Fig. 8(b)) was simulated with a bandwidth of 500Hz. The voltage from the *PLL* is obtained by using the reference angle and the amplitude of the supply voltage into the *dq* to *abc* transformation.

5. IMPLEMENTATION OF SHUNT ACTIVE FILTER

The implementation scheme of shunt filter can be viewed in Figure 3.

5.1. Signal Conditioning

The current and voltage signals are sensed using Halleffect sensors and instrumentation amplifiers. This acquisition system was built to decrease the amplitude of the signal references to a range between zero and 3 volts and the output signals have the additional characteristic of a low output impedance with the objective of wasting as little time as possible in the Analogue-Digital conversion.

5.2. Digital Signal Processor

A *DSP* is a specific device to manipulate digital data that are measured by Analogue-Digital converters with the objective of processing these data as quickly as possible to generate output signals to control systems in real time operation.

The *TMS320F2812* used to implement the active filter can be classified as Digital Signal Controller (*DSC*). Combining the computational capacity of *DSP* with memory and peripherals like AD converters and event managers in one single device, it is possible to have an effective solution on

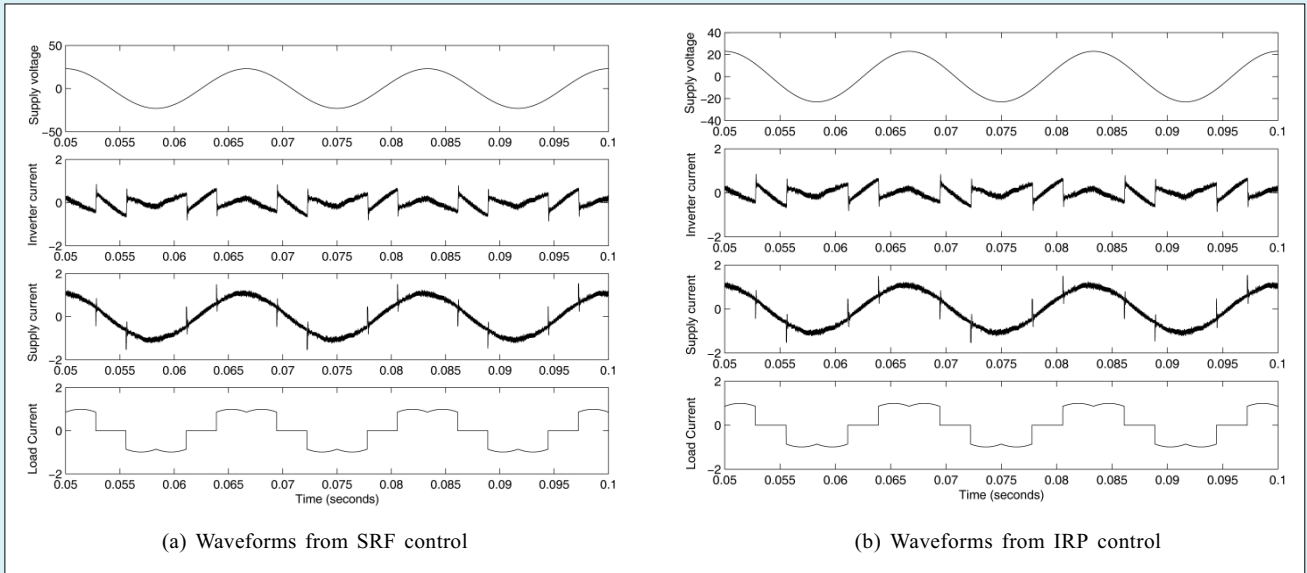


Fig. 6. Simulation results with undistorted supply voltage

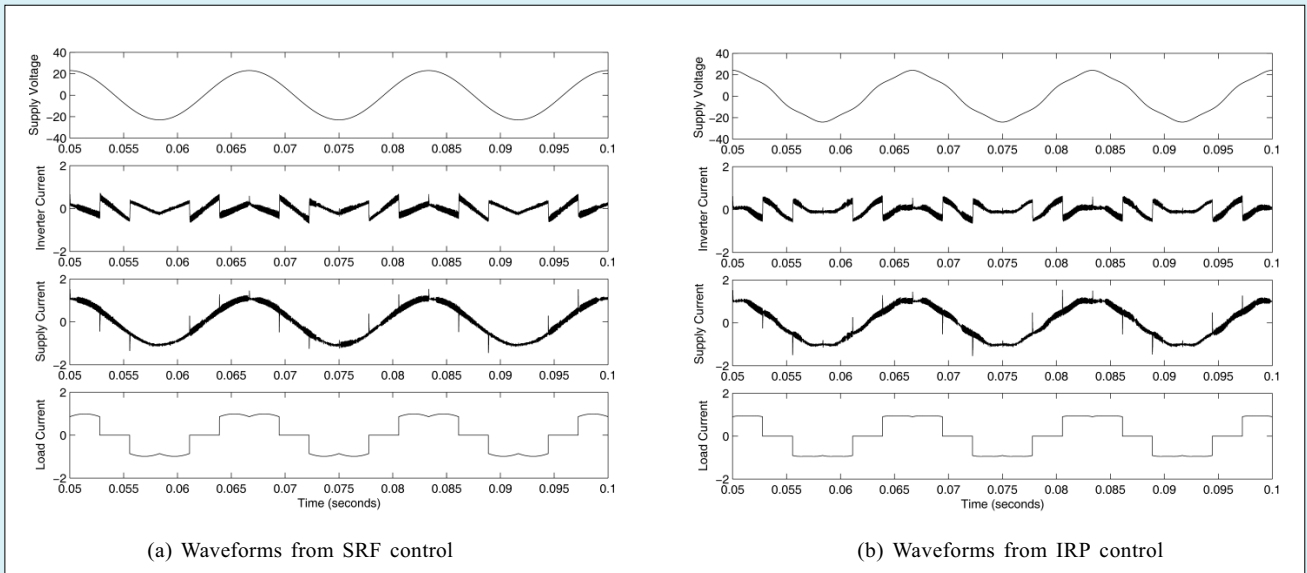


Fig. 7. Simulation results with distorted supply voltage

digital control in real-time. In a general way the *DSC* can be considered a *DSP* device.

The *DSP* used in the implementation of the shunt active filter system was a fixed-point *DSP* with capacity of processing 150 Millions of Information Per Second (*MIPS*) using fixed-point with words of 32 bits. All operations in the control strategy are done in Q.15 notation, except the PI controllers routine which are implemented in Q.22.

The architecture of this kind of *DSP* is based on *Harvard* architecture, so two independent buses systems exist: one for the program memory and other for data memory. Hence it facilitates the access to the memory map, decreasing the time to access the memory. The memory space is divided in program and data space. There are different types of memory: flash, RAM (*SARAM*), expanded *SARAM* and boot ROM memory.

For the implementation of the shunt filter it is necessary to use 7 of 16 channels of the Analog to Digital Conversion

(*ADC*) module [16]. Each signal spends at least 200ns to be converted. The *ADC* module has precision of 12 bits and it was configured in cascaded mode, which means that all channels were converted one by one and once a conversion is completed, the selected channel value is stored in the respective result register.

Once the AD conversion is concluded, a low-pass Finite Impulse Response (*FIR*) filter of second order is used to separate the harmonics from the fundamental component of current. This filtering is done using the *dq* components, in such way that it is needed only to filter the dc component of the signal with a cutoff frequency of approximately 20Hz.

The switching frequency of the system is 20KHz and a counter with an interrupt routine [17] was used to give a basis of time to impose this frequency. It means that in each 50μs, the output registers of *DSP* need to be changed. The event manager [18] is responsible for the generation of this basis of time to calculate the switches duty cycle. This

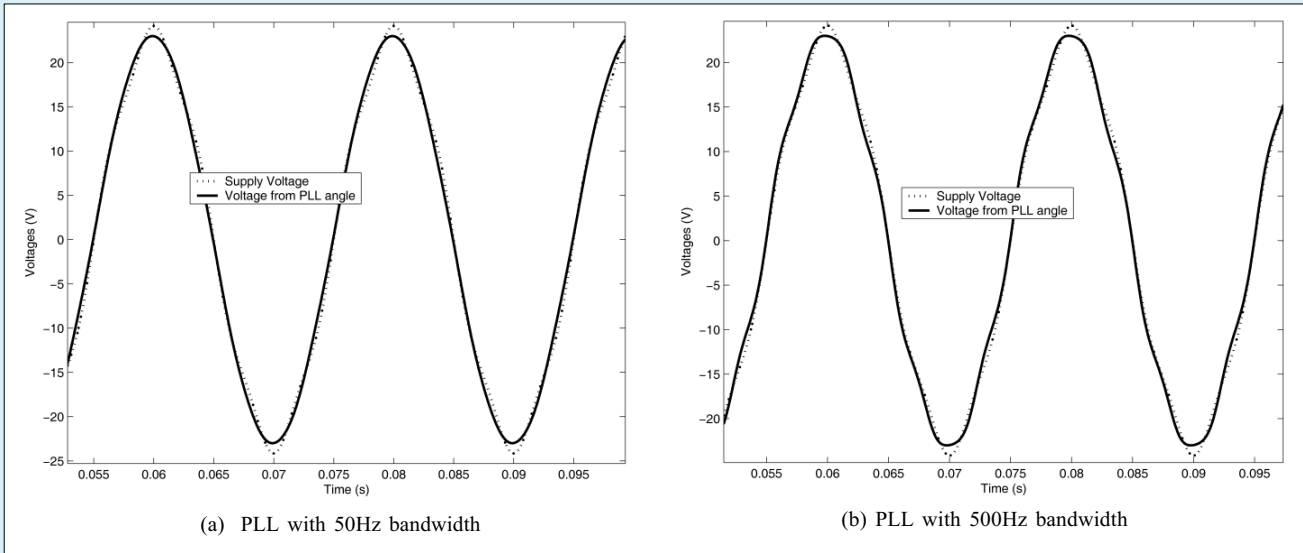


Fig. 8. PLL response for two different bandwidth

peripheral is able to produce hardware signals directly from an internal time event.

The interrupt system of *DSP* consists of 16 types of interrupts; two of them are non-maskable and 14 are maskable. Each 16 types of interrupts have different priorities.

The interrupt called *ADCINT* (maskable hardware interrupt) was used to impose the frequency to the system. This routine is always initialized in the end of the last signal conversion and a counter called *TxCNT* is responsible for making sure that the AD conversion will be started at each $50\mu s$.

The J-TAG peripheral allows watching variables while the code is running in real-time, without any delay to the control code. Figures 9 and 10 were captured using J-TAG peripheral.

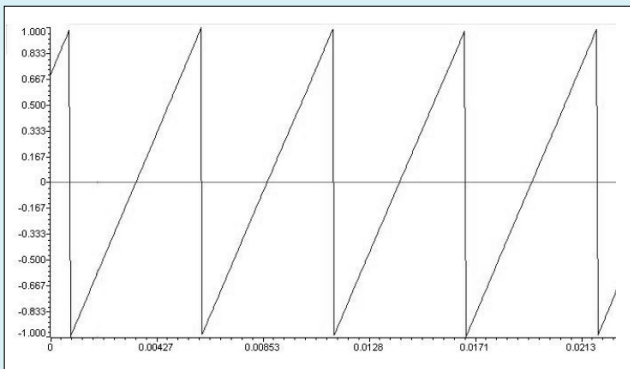


Fig. 9. Phased Locked Loop angle

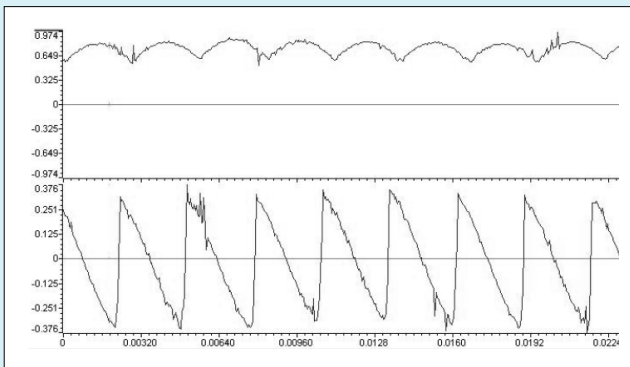


Fig. 10. Load currents in *dq* coordinates

Figure 9 shows the *PLL* angle for the *dq* reference frame orientation. The vertical scale is normalized by the factor π . Figure 10 shows the waveforms (i_d and i_q) of the load current in *dq* coordinates. These waveforms are normalized by a factor of 3.3.

5.3. Pulse Width Modulation

Space vector modulation is nowadays the most used *PWM* technique to control inverters. In the space vector *PWM* (*SV PWM*), each phase is switched in sequence by switching only one inverter leg at each transition from one state to the next one. One possibility to reduce the number of switching is to use the two-phase modulation in which only two phases are modulated while the third phase is clamped to the positive (*DPWMMAX*) or negative (*DPWMMIN*) dc rail [19].

Space vector modulation techniques can also be implemented by using digital scalar *PWM*. In this approach, nonsinusoidal modulating waveforms are introduced in a simple way. In digital scalar *PWM* the split and distribution of the zero space vectors duration $V_0(t_{01})$ and $V_7(t_{02})$, inside the sampling interval, can be represented by the apportioning factor $\mu = t_{01} / (t_{01} + t_{02})$ [20]. When $0 < \mu < 1$ the modulation is known as continuous modulation. The case $\mu = 0.5$ is equivalent to *SV PWM*. When $\mu = 0$ (*DPWMMAX*) or $\mu = 1$ (*DPWMMIN*) the modulation is known as discontinuous modulation. Because of the simple implementation, the digital scalar *PWM* with $\mu = 0.5$ is used to control the inverter.

5.4. Experimental results

The experimental results using the *SRF* control are shown in Figure 11 and Figure 12. In Figure 11 are shown (from top to bottom): the supply voltage, the supply current and the load current. The supply voltage and current are in phase as expected. In Figure 12 are shown (from top to bottom): the inverter current, the inverter plus load current and the load current. Each $100mV$ represents $1A$ in current scale. Comparing the experimental results with simulation results it can be seen that they are very similar results.

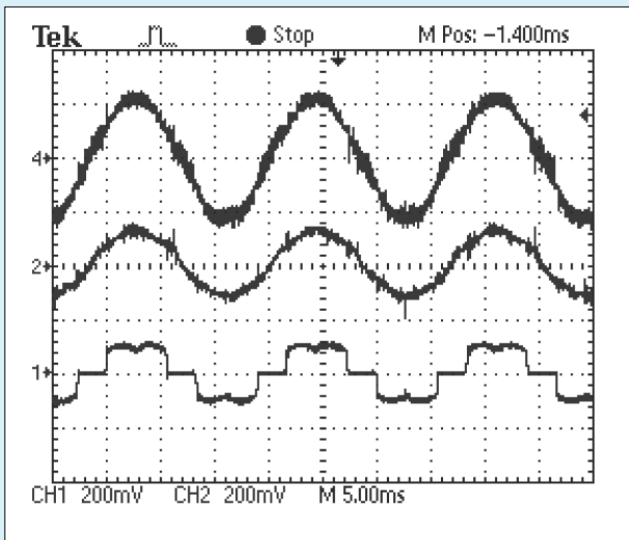


Fig. 11. Experimental waveforms. From top to bottom: the supply voltage, the supply current and the load current

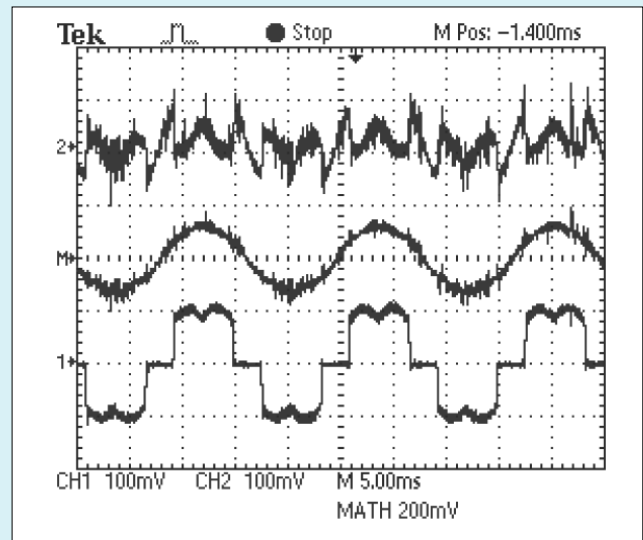


Fig. 12. Experimental waveforms. From top to bottom: the inverter current, the inverter plus load current and the load current

VI. CONCLUSION

The active filters are becoming a cost effective solution to eliminate harmonics. Using simulation results, it is possible to make a comparative study of different possibilities of control for active filters. A synchronous reference frame based controller is compared to an instantaneous reactive power based controller. The controllers have been tested under balanced supply voltage conditions. In presence of undistorted supply voltage, the controllers work very well, but in presence of distorted supply voltage, the synchronous reference frame method presents better performance than the instantaneous reactive power method. Therefore the synchronous reference frame method is chosen to control the three-phase inverter. To evaluate the shunt active filter, experimental results have been obtained by using a digital signal processor. The processor together with its memory and peripherals, like AD converters and event managers, constitute an effective solution to implement the digital control in real time. The implemented system provides current harmonics compensation and reactive power compensation simultaneously.

ACKNOWLEDGMENT

The authors would like to thank CNPq and CAPES for its financial support.

REFERENCES

- Bhattacharya S., Divan D.M. and Banerjee B.: *Active Filter Solutions for Utility Interface*. Industrial Electronics, 1995. ISIE '95, Proc. of the IEEE International Symposium on, Vol. 1 pp 53-63.
- Singh B., Al-Haddad K. and Chandra A.: *A Review of Active Filters for Power Quality Improvement*. IEEE/Trans. Ind. Elect. 1999, 5, 46, pp 960-971.
- Mendalek N. and Al-Haddad K.: *Modeling and nonlinear control of shunt active power filter in the synchronous reference frame*. Harmonics and Quality of Power, 2000, Proc. Ninth International Conference, 5, 1, pp 30-35.
- Bhattacharya S., Frank T.M., Divan D.M. and Banerjee B.: *Active filter System Implementation*. IEEE Ind. Appl. Magazine, 1998, 4, 5 pp 47-63.
- Fujita H. and Akagi H.: *The Unified Power Quality Conditioner: The integration of Series- and Shunt- Active Filters*. IEEE/Trans. Power. Elec. 1998, 2, 13, pp 315-322.
- Peng F.Z., Akagi H. and Nabae A.: *A Novel Harmonic Power Filter*. IEEE/PESC, 1988, pp 1151-1158.
- Fujita H. and Akagi H.: *A New Approach to Harmonic Compensation in Power Systems- A Combined System of Shunt Passive and Series Active Filters*. IEEE/Trans. Ind. Appl. 1990, 6, 26, pp 983-989.
- Fujita H. and Akagi H.: *A Practical Approach to Harmonic Compensation in Power Systems- Series Connection of Passive and Active Filters*. IEEE/Trans. Ind. Appl., 1991, 6, 27, pp 1020-1025.
- Fujita H. and Akagi H.: *A New Power Line Conditioner for Harmonic Compensation in Power Systems*. IEEE/Trans. Power. Del., 1995, 3, 10, pp 1570-1575.
- Mendalek N. and Al-Haddad K.: *Nonlinear control strategy applied to a shunt active power filter*. Power Electronics Specialists Conference, 2001. PESC. 2001 IEEE 32nd Annual, 4, pp 1877-1882.
- Akagi H., Kanagawa Y. and Nabae A.: *Generalized Theory of Instantaneous Reactive Power in Three-Phase Circuits*. Int. Conf. Power Electronis, Tokio, 1983.
- Akagi H., Kanagawa Y. and Nabae A.: *Instantaneous Reactive Power Compensator Comprising Switching Devices Without Energy Storage Components*. IEEE/Trans. Ind. Appl., 1984, 2, Vol IA-20.
- Watanabe E.H., Stephan R.M. and Aredes M.: *New Concepts of Instantaneous Active and Reactive Power in Electrical Systems with Generic Loads*. IEEE/Trans. power. Deliv., 1993, 2, 8.
- Bhattacharya S. and Divan D.: *Synchronous Frame Based Controller Implementation for a Hybrid Series Active Filter system*. In Conf. Rec. IEEE-IAS Annu. Meeting, 1995, pp 2531-2540.
- Kaura V. and Blasko V.: *Operation of a Phase Locked Loop System Under Distorted Utility Conditions*. Trans. Ind. Appl., 1997, 33, 1, pp 58-63.
- Texas Instruments: *TMS320F28x Analog-to-Digital Converter (ADC) Peripheral Reference guide*. Literature number: SPRU060, June 2002.
- Texas Instruments: *TMS320F28x System Control and Interrupts Peripheral Reference guide*. Literature number: SPRU078, May 2002.
- Texas Instruments: *TMS320F28x Event Manager (EV) Peripheral Reference guide*. Literature number: SPRU065, May 2002.
- Hava A.M., Kerkman R.J. and Lipo T.A.: *Simple Analytical and Graphical Tools for Carrier Based PWM Methods*. IEEE Power Electronic Specialists Conference, 1997, pp. 1462-1471.
- Jacobina C.B., Lima A.M.N., da Silva E.R.C., Alves R.N.C. and Seixas P.F.: *Digital Scalar Pulse-width Modulation: A Simple Approach to Introduce Non-Sinusoidal Modulating Waveforms*. IEEE/Trans. Power Elec., 2001, 3, 16, pp 351-359.



Leonardo Rodrigues Limongi

was born in Recife, Brazil, in 1978. He received the B.S. and M.S. degrees in electrical engineering from the Federal University of Pernambuco, Recife, Brazil, in 2004 and 2006, respectively. He is currently working toward the Ph.D. degree in electrical engineering in the Politecnico di Torino, Torino, Italy. His research interests are the design and development of DSP-based advanced control systems in the fields of power electronics and power conditioning systems.



Marcelo Cabral Cavalcanti

was born in Recife, Brazil, in 1972. He received the B.S. degree in electrical engineering in 1997 from the Federal University of Pernambuco, Recife, Brazil, and the M.S. and Ph.D. degrees in electrical engineering from the Federal University of Campina Grande, Campina Grande, Brazil, in 1999 and 2003, respectively. Since 2003, he has been at the Electrical Engineering and Power Systems Department, Federal

University of Pernambuco, where he is currently a Professor of Electrical Engineering. His research interests are power electronics, renewable energy systems and power quality.



Francisco de Assis dos Santos Neves

was born in Campina Grande, Brazil, in 1963. He received the B.S. and M.S. degrees in electrical engineering from the Federal University of Pernambuco, Recife, Brazil, in 1984 and 1992, respectively and the Ph.D. degree in electrical engineering in 1999 from the Federal University of Minas Gerais, Belo Horizonte, Brazil. Since 1993, he has been at the Electrical Engineering and Power

Systems Department, Federal University of Pernambuco, where he is currently a Professor of Electrical Engineering. His research interests are power electronics, renewable energy systems and power quality.



Gustavo Medeiros de Souza Azevedo

was born in Belo Jardim, Brazil, in 1981. He received the B.S. degree in electrical engineering in 2006 from the Federal University of Pernambuco, Recife, Brazil, where he is currently working toward the M.S. degree. His research interests are power electronics and renewable energy systems.